



LAWRENCE  
LIVERMORE  
NATIONAL  
LABORATORY

# Using the X-ray free-electron laser to drive a photo-pumped helium-like neon X-ray laser at 23 nm

J. Nilsen, H. A. Scott

October 13, 2010

High Energy Density Physics

## **Disclaimer**

---

This document was prepared as an account of work sponsored by an agency of the United States government. Neither the United States government nor Lawrence Livermore National Security, LLC, nor any of their employees makes any warranty, expressed or implied, or assumes any legal liability or responsibility for the accuracy, completeness, or usefulness of any information, apparatus, product, or process disclosed, or represents that its use would not infringe privately owned rights. Reference herein to any specific commercial product, process, or service by trade name, trademark, manufacturer, or otherwise does not necessarily constitute or imply its endorsement, recommendation, or favoring by the United States government or Lawrence Livermore National Security, LLC. The views and opinions of authors expressed herein do not necessarily state or reflect those of the United States government or Lawrence Livermore National Security, LLC, and shall not be used for advertising or product endorsement purposes.

# Using the X-ray free-electron laser to drive a photo-pumped helium-like neon X-ray laser at 23 nm

Joseph Nilsen and Howard A. Scott

*Lawrence Livermore National Laboratory, Livermore, CA 94551*

**Abstract.** Nearly four decades ago resonantly photo-pumped laser schemes based on hydrogen-like and helium-like ions were proposed for producing X-ray lasers. Demonstrating these schemes has proven to be elusive because of the difficulty of finding an adequate resonance between a strong pump line and a line in the laser plasma that drives the laser transition. Even when a good resonance is found, a second challenge has been to simultaneously create the pump and laser plasma in close proximity so as to allow the pump line to transfer its energy to the laser material. With the construction of the X-ray free electron laser (X-FEL) at the SLAC Linac Coherent Light Source (LCLS) researchers now have a very bright tunable X-ray laser source that can be used to replace the pump line in previously proposed laser schemes and allow one to study the physics and feasibility of photo-pumped laser schemes. In this paper we model the sodium-pumped neon X-ray laser scheme that was proposed and studied many years ago by replacing the Na He- $\alpha$  pump line at 1127 eV with the X-FEL. Using the X-FEL to photo-ionize Ne down to He-like Ne and then photo-pump the He- $\gamma$  line we predict gains greater than  $400\text{ cm}^{-1}$  on the  $4f - 3d$  transition at 23.1 nm in He-like Ne. The  $4d - 3p$  line at 23.16 nm and the  $4p - 3s$  line at 22.27 nm are also predicted to lase strongly.

**Keywords:** X-ray laser; X-FEL; LCLS; photo-pumping; Helium-like Neon

## **Corresponding author:**

Joseph Nilsen

Lawrence Livermore National Laboratory

P.O. Box 808, L-38

Livermore, CA 94551-0808

Phone: 1-925-422-4766

FAX: 1-925-422-8040

Email: nilsen1@llnl.gov

## 1 Introduction

From the earliest days of lasers, resonantly photo-pumped laser schemes using H-like and He-like ions have been proposed for producing X-ray lasers [1]. Demonstrating these schemes in the laboratory has proven to be very elusive. A major challenge has been the difficulty of finding a good resonance between a strong pump line and a line in the laser plasma that drives the laser transition. After finding a good resonance, a second challenge has been to create both the pump and laser plasma in close proximity so as to allow the pump line to transfer its energy to the laser material. With the availability of the X-FEL at LCLS [2] there now exists a tunable X-ray laser source that can be used to replace the pump line in previously proposed laser schemes and allow researchers to study the physics and feasibility of photo-pumped laser schemes. In this paper we model the Na-pumped Ne X-ray laser scheme that was proposed and studied many years ago by replacing the Na He- $\alpha$  pump line at 1127 eV (or 1.10027 nm) with the X-FEL at LCLS. We predict gain on the 4f – 3d transition at 23.1 nm in He-like Ne that is orders of magnitude larger than the gains predicted [3] two decades ago using the Saturn pulsed power machine at Sandia National Laboratory to create the Na pump line. The 4d – 3p line at 23.16 nm and the 4p – 3s line at 22.27 nm are also predicted to lase strongly. Table 1 shows all the resonantly photo-pumped H and He-like schemes that could lase on the 4f – 3d lines that were identified many years ago but which have not yet been demonstrated. A good resonance was defined as the lines in the pump and laser material overlapping within one part in a thousand. The X-FEL can now replace any of these pump lines and enable us to study these lasing schemes. With the X-FEL we are no longer restricted to studying these accidental resonances but can photo-pump the Ly- $\gamma$  or He- $\gamma$  lines in other nearby ions.

Over the years many other photo-pumped schemes have been proposed in iso-electronic sequences such as Li-like, Ne-like, Na-like, and Ni-like [4 - 8]. With the X-FEL we now have a tool that we can use to study all of these schemes. We are no longer constrained by finding the accidental resonances in nature. In addition the X-FEL can be used to photo-ionize inner shell electrons in materials such as Ne gas and create gain without directly photo-pumping a line [9]. The X-FEL enables researchers to study many of the resonant and non-resonant photo-pumping schemes that have been proposed for many years. With the advances in computational capability since many of these schemes were proposed we also have much better tools to model these schemes.

## 2 The X-FEL beam characteristics at LCLS

With the availability of the X-FEL at the LCLS facility we examined the characteristics [10] of the X-FEL output to see if it would be suitable for photo-pumping X-ray laser

schemes. To drive an X-ray laser we assume the X-FEL would longitudinally pump a volume of X-ray laser plasma of a given length from one end of the plasma, as shown in Fig. 1. The X-ray laser would be emitted from the opposite end of the plasma in the same direction as the X-FEL beam. The basic feature of the X-FEL is that it can produce a tunable X-ray source that extends from 800 to 8500 eV in energy or 1.5 nm to 0.15 nm in wavelength. It operates at a 120 Hz repetition rate with approximate output of  $10^{12}$  photons per pulse. The beam has a spectral bandwidth of 0.1% of the fundamental, pulse duration of 100 - 200 fs, and an unfocused spot size of 400  $\mu\text{m}$  square. The beam can be focused down to a 1- $\mu\text{m}$  square using X-ray optics. The beam can be rapidly tuned over 3% of the fundamental energy by adjusting the electron beam energy. Using the unfocused beam [11] we predicted that the photo-ionization rate of Ne gas is about 10 per  $\mu\text{sec}$ , which is much too slow for using the X-FEL to photo-ionize Ne gas down to the He-like iso-electronic sequence. In that case a separate optical laser would be required to heat and ionize the plasma to He-like Ne.

In this paper we look at the case of a focused X-FEL beam with a 1- $\mu\text{m}$  spot size and 100 fs pulse duration. Using these numbers gives a spectral intensity  $I_\epsilon = 1.6 \times 10^{17} \text{ W} / (\text{eV cm}^2)$ . The line strength of the X-FEL beam in photons per mode  $n_\epsilon = 1.579 \times 10^{-5} I_\epsilon / \epsilon^3$  where  $\epsilon$  is the photon energy in eV. Looking at some typical photon energies  $n_\epsilon = 1765$  at 1127 eV and drops to 9.45 at 6442 eV for the focused beam. For a photo-pumped laser scheme the beam strength in photons per mode is the ratio of the stimulated rate to the spontaneous rate. This is approximately the same as the maximum fractional population divided by the statistical weight of the level being pumped when the beam strength is much less than one. When the beam strength exceeds one it mean the stimulated rate is much larger than the spontaneous rate and the two levels will be locked into equilibrium with similar populations per statistical weight. The statistical weight of a level is  $2J + 1$  where  $J$  is the total angular momentum of the level.

### 3. Description of the He-like Ne X-ray laser scheme

One of the earliest resonantly photo-pumped scheme that was studied and tried experimentally was the Na-pumped Ne scheme that used the He- $\alpha$  line of Na to photo-pump the He- $\gamma$  line of Ne and create gain on several  $n = 4$  to  $n = 3$  transitions in He-like Ne. Figure 2 shows the three principal laser lines that were predicted to have gain, the 4f – 3d line at 23.11 nm, the 4d – 3p line at 23.16 nm, and the 4p – 3s line at 22.27 nm. The 4p – 3s line lases directly from the 4p level that is being photo-pumped. However, it is important to understand that the other two laser lines depend on collisional excitation to transfer population from the 4p to 4d to 4f states. Since these states are very close in energy they tend to equilibrate very quickly if the density of the plasma is high enough. Using a conversion factor of  $hc = 1239.842 \text{ eV nm}$ , the 23.11 nm line has a photon energy of 53.6 eV.

We should point out that one could also photo-pump the He- $\beta$  line and look for gain on the  $n = 3 - n = 2$  transitions, which have smaller gains but shorter wavelengths. Resonances for

photo-pumping Ly- $\beta$  and He- $\beta$  lines are discussed in Ref. 1 and those systems could also be pursued using the X-FEL as a line source.

To model this system we used an ion density of  $10^{18} \text{ cm}^{-3}$  for the Ne gas, which is the same as used in the Saturn pulsed power experiments that were done many years ago [3]. Because of the complexity of the atomic model for near neutral sequences the calculation were started in the O-like Ne iso-electronic sequence with an electron temperature of 1 eV and an ion temperature of 0.025 eV. In He-like Ne the atomic model had 252 levels including doubly excited states up to 2p5f while O-like Ne has 1537 levels. The CRETIN code [12] was used to model the kinetics in one dimension (1D). We created an input file that represented the monochromatic X-FEL beam at 1127 eV with a full width of 1.1 eV using a square pulse shape and a 100 ps full-width half maximum (FWHM) temporal duration Gaussian pulse. The pulse peaks at 200 ps in the various figures. Under these conditions the peak photo-ionization rate for the Ne plasma in the Li-like sequence is  $5 \text{ psec}^{-1}$ . Figure 3 shows the ionization fraction of the various iso-electronic sequences versus time. One observes that the plasma quickly reaches 40% He-like and 55% Li-like shortly after the peak of the pulse. For photo-pumped systems the first goal is to create a large population in the He-like Ne ground state that is being pumped. Given the large Li-like population it appears that we are not over-ionizing this plasma and would have even higher gain if we could ionize more of the Li-like.

Figure 4 shows the electron temperature of the Ne plasmas versus time. The plasma quickly reaches an electron temperature of 208 eV while the ion temperature stays near room temperature and only slowly doubles to 0.05 eV by 1100 ps. For these short pulse driven low-density plasmas the ions stay very cold and are decoupled from the electrons. This means the Doppler width is quite small and the collisional broadening of the laser line will dominate the laser line-width.

Another important issue to understand is the fractional populations divided by the statistical weight of the upper laser states and the ground state in He-like Ne. The lower laser states have very small populations initially. Figure 5 shows the fractional populations divided by the statistical weight versus time for the He-like ground state and three of the upper laser levels. The statistical weight of a level is  $2J + 1$  where  $J$  is the total angular momentum of the level. One can observe how the 1s and 4p levels are locked together by the strong X-FEL and then diverge as the X-FEL turns off. As the population of the 4p level decays one observes the populations of the 4d and 4f levels rise as collision processes try to equilibrate the populations of these levels. The calculation is done so that the X-FEL pulse peaks at 200 fsec on the time axis.

Figure 6 shows the predicted gain for the three strongest laser lines in He-like Ne. The dominant line is the 4f – 3d transition that has a peak gain of  $438 \text{ cm}^{-1}$  at 1067 fs. This line has a FWHM gain duration of 1840 fs. In contrast the 4d – 3p line has a peak gain of  $270 \text{ cm}^{-1}$  at 496 fs and the 4p – 3s line has a peak gain of  $333 \text{ cm}^{-1}$  at 301 fs. The 4f – 3d gain peaks almost 900 fs after the peak of the X-FEL drive pulse because of the time needed for electron collisions to transfer population from the 4p level via the 4d level. One observes how the 4p –

3s line peaks much closer to the peak of the X-FEL drive beam. With these high gains a plasma length of 0.1 cm should be more than sufficient to obtain saturated output for the laser lines. We also predict gain of  $80 \text{ cm}^{-1}$  on the  $4p - 2s$  line that we estimate to have a wavelength near 5.9 nm.

If we look at the absorption coefficient for the  $1s - 4p$  He-like Ne line that is being photo-pumped, as shown in Fig. 7, it has a value of  $0.24 \text{ cm}^{-1}$  at 200 fs, the peak of the X-FEL pump pulse. It remains less than  $1 \text{ cm}^{-1}$  until 300 fs, which is when the X-FEL pump is mostly over. This suggests that the X-FEL could pump a 1-cm length of plasma without too much attenuation. This would allow gain-length products greater than 400. Typically X-ray lasers need 15 – 20 gain-lengths to reach saturation, so Ne plasmas less than 0.1-cm in length could potentially achieve saturated output on all three of the strong  $n = 4 - n = 3$  laser lines .

## 4 Conclusions

From the earliest days of laser research H-like and He-like resonantly photo-pumped laser schemes have been proposed for producing X-ray lasers but have never been demonstrated. A major challenge has been the difficulty of finding an adequate resonance between a strong pump line and a line in the laser plasma that drives the laser transition. Given a good resonance, a second challenge has been to create both the pump and laser plasma in close proximity so as to allow the pump line to transfer its energy to the laser material. With the availability of the X-FEL at LCLS we now have a tunable X-ray laser source that can be used to replace the pump line in previously proposed laser schemes and allow researchers to study the physics and feasibility of photo-pumped laser schemes. In this paper we model the Na-pumped Ne X-ray laser scheme that was proposed and studied many years ago by replacing the Na He- $\alpha$  pump line at 1127 eV with the X-FEL at LCLS to drive the He- $\gamma$  transition in He-like Ne. We predict gain greater than  $400 \text{ cm}^{-1}$  on the  $4f - 3d$  transition at 23.11 nm in He-like Ne that would allow it to reach saturated lasing output in a plasma less than 0.1-cm length. The  $4d - 3p$  line at 23.16 nm and the  $4p - 3s$  line at 22.27 nm are also predicted to lase strongly. Given the tunable nature of the X-FEL we are no longer restricted to studying photo-pumping in just the materials that have accidental resonances with strong pump lines but we can now study any ion of interest that falls within the spectral range of the X-FEL. The X-FEL enables researchers to study many of the resonant and non-resonant photo-pumping schemes that have been proposed for many years. In addition to looking for gain and lasing the X-FEL can also be used to study the kinetics of these laser systems by observing the dynamic evolution of the fluorescent lines.

**Acknowledgements.** This work was performed under the auspices of the U.S. Department of Energy by Lawrence Livermore National Laboratory under Contract DE-AC52-07NA27344.

## References

1. Joseph Nilsen, James H. Scofield, and Elaine A. Chandler, "Reinvestigating the Early Resonantly Photo-Pumped X-ray Laser Schemes," *Appl. Opt.* **31**, 4950 – 4956 (1992).
2. See SLAC National Accelerator Laboratory web site <http://lcls.slac.stanford.edu/>
3. Joseph Nilsen and Elaine Chandler, "Analysis of the resonantly photo-pumped Na-Ne X-ray laser scheme," *Phys. Rev. A* **44**, 4591 – 4598 (1991).
4. Joseph Nilsen, "A Ne-like Fe laser resonantly photo-pumped by Ne X Ly- $\alpha$  radiation," *J. Quant. Spectrosc. Radiat. Transfer* **46**, 547 - 556 (1991).
5. Joseph Nilsen, "Resonantly Photo-Pumped Na-like X-ray Lasers," *J. Quant. Spectrosc. Radiat. Transfer* **47**, 171 - 177 (1992).
6. Joseph Nilsen, "Resonantly Photo-Pumped Li-like X-ray Lasers," *Appl. Opt.* **31**, 4957 - 4961 (1992).
7. V. Yu. Politov, P. A. Loboda, V. A. Lykov, and Joseph Nilsen, "A 64 Å Ne-like Ge X-ray laser resonantly photo-pumped by Ly- $\alpha$  Mg radiation," *Opt. Comm.* **108**, 283 - 288 (1994).
8. Joseph Nilsen, "Ni-like X-ray lasers resonantly photo-pumped by Ly- $\alpha$  radiation," *Phys. Rev. Lett.* **66**, 305 – 308 (1991).
9. Nina Rohringer and Richard London, "Atomic inner-shell x-ray laser pumped by an x-ray free-electron laser," *Phys. Rev. A*, **80**, 013809 (2009).
10. Richard (Dick) W. Lee from LLNL – private communications.
11. Joseph Nilsen, "Using short pulse lasers to drive X-ray lasers." *SPIE Proceedings 7451 - Soft X-ray Lasers and Applications VIII*, edited by Gregory J. Tallents and James Dunn (SPIE Press, Bellingham, 2009), pp. 74510N-1-8
12. Howard A. Scott, "Cretin - a radiative transfer capability for laboratory plasmas," *JQSRT* **71**, 689 - 701 (2001).



Table 1. Resonantly photo-pumped laser schemes with 4f – 3d lasing in H and He-like ions							
Pump Line		$\lambda_p$ (nm)	Absorbing Line		$\lambda_A$ (Å)	$\Delta\lambda_p/\lambda_p$ (%)	$\lambda_L$ (nm)
Na	He- $\alpha_S$	1.1003	Ne	He- $\gamma_S$	1.1000	0.022	23.1
K	Ly- $\alpha_2$	0.33521	Cl	Ly- $\gamma_2$	0.33511	0.029	6.48
Cr	He- $\alpha_T$	0.21925	Sc	Ly- $\gamma_2$	0.21917	0.036	4.25
Mn	Ly- $\alpha_1$	0.19247	V	He- $\gamma_S$	0.19255	0.040	3.87
Cu	Ly- $\alpha_1$	0.14253	Fe	Ly- $\gamma_2$	0.14253	0.006	2.77
Sr	Ly- $\alpha_2$	0.082708	Se	Ly- $\gamma_1$	0.082765	0.069	1.62
Nb	He- $\alpha_S$	0.072175	Rb	He- $\gamma_T$	0.072143	0.044	1.44

## Figure Captions

**Fig. 1.** Schematic of the X-FEL beam longitudinally pumping a length of plasma from one end. The X-ray laser beam is emitted in the same direction from the opposite end.

**Fig. 2.** Energy level diagram for the Na-pumped Ne X-ray laser scheme.

**Fig. 3.** Fractional population of Ne iso-electronic sequences versus time. The intensity of the X-FEL peaks at 200 fs on this time scale.

**Fig. 4.** Electron temperature of Ne plasma versus time. The intensity of the X-FEL peaks at 200 fs on this time scale.

**Fig. 5.** Fractional population of He-like Ne ground state and upper laser state levels divided by the statistical weights ( $2J+1$ ) versus time. The intensity of the X-FEL peaks at 200 fs on this time scale.

**Fig. 6.** Gain of three  $n=4 - n=3$  laser transitions of He-like Ne versus time. The intensity of the X-FEL peaks at 200 fs on this time scale.

**Fig. 7.** Absorption coefficient of the  $1s - 4p$  He-like Ne line that is photo-pumped versus time. The intensity of the X-FEL peaks at 200 fs on this time scale.

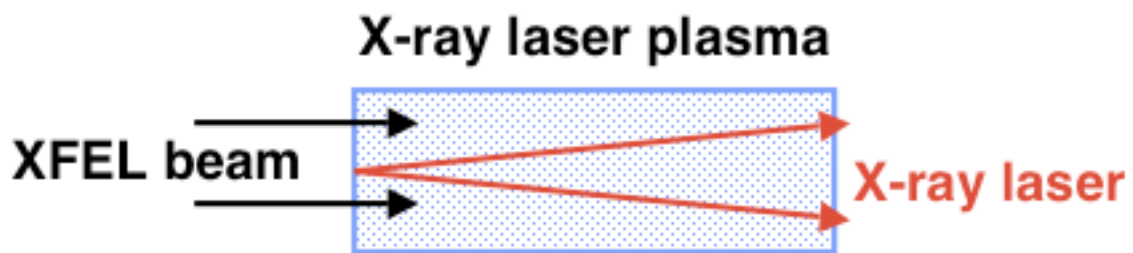


**Fig. 1.** Schematic of the X-FEL beam longitudinally pumping a length of plasma from one end. The X-ray laser beam is emitted in the same direction from the opposite end.

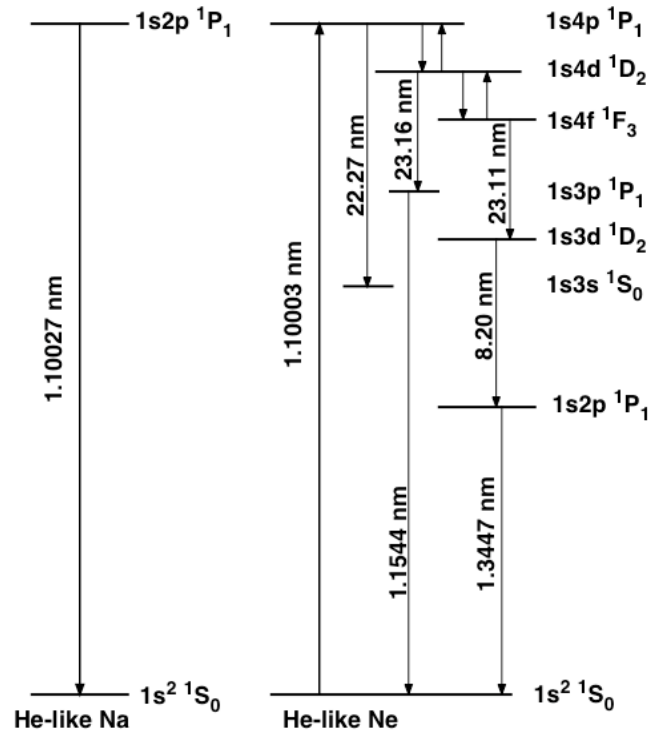


**Fig. 2.** Energy level diagram for the Na-pumped Ne X-ray laser scheme.

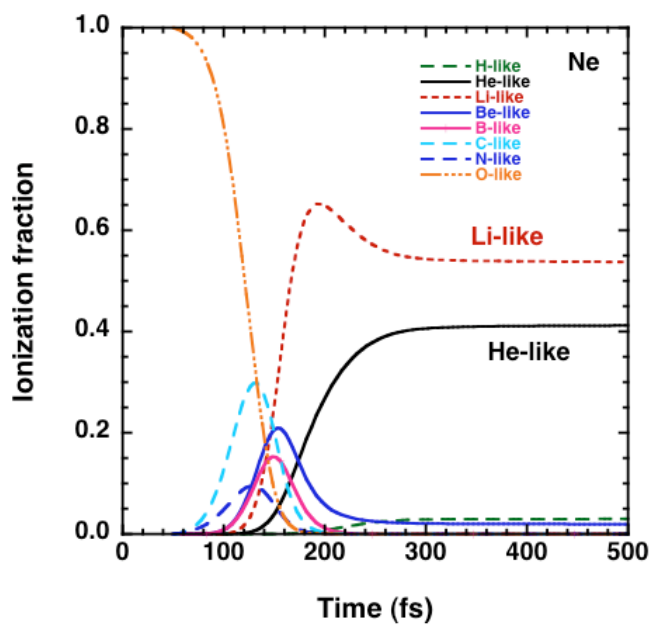


**Fig. 3.** Fractional population of Ne iso-electronic sequences versus time. The intensity of the X-FEL peaks at 200 fs on this time scale.

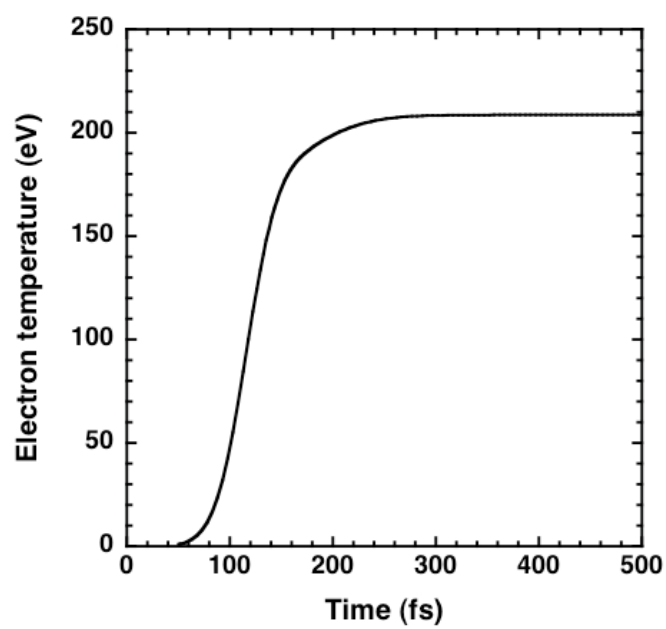


**Fig. 4.** Electron temperature of Ne plasma versus time. The intensity of the X-FEL peaks at 200 fs on this time scale.

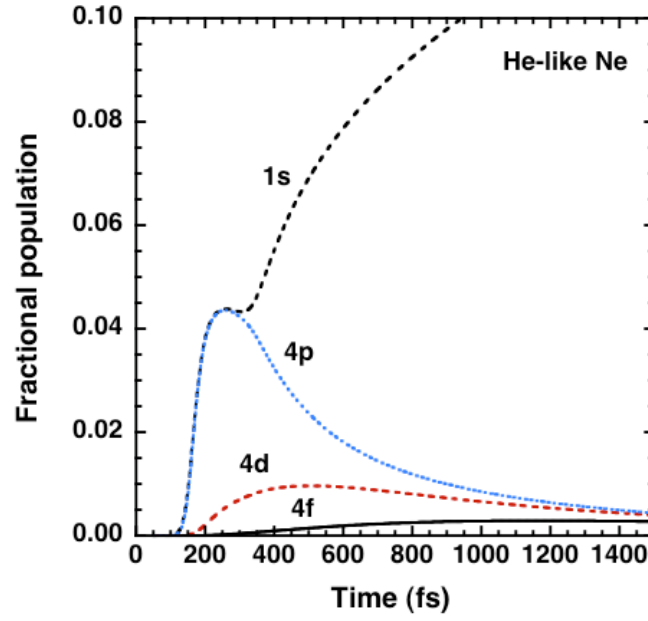


**Fig. 5.** Fractional population of He-like Ne ground state and upper laser state levels divided by the statistical weights ( $2J+1$ ) versus time. The intensity of the X-FEL peaks at 200 fs on this time scale.

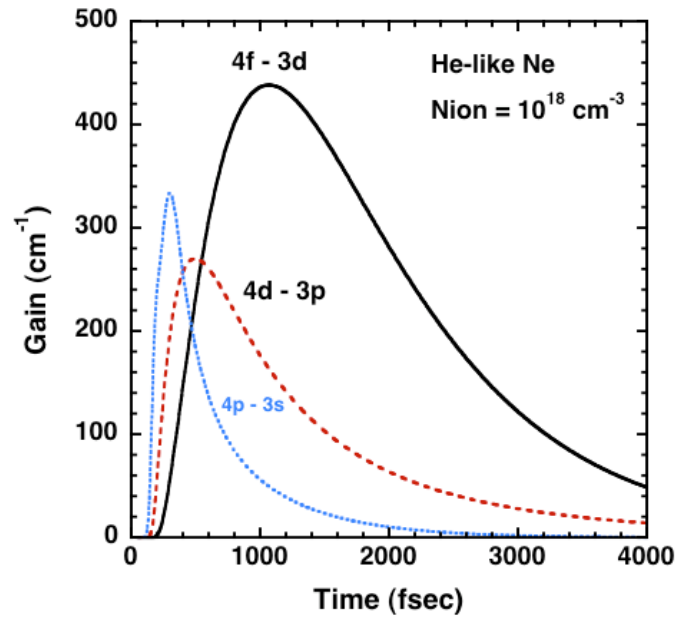


**Fig. 6.** Gain of three  $n=4 - n=3$  laser transitions of He-like Ne versus time. The intensity of the X-FEL peaks at 200 fs on this time scale.



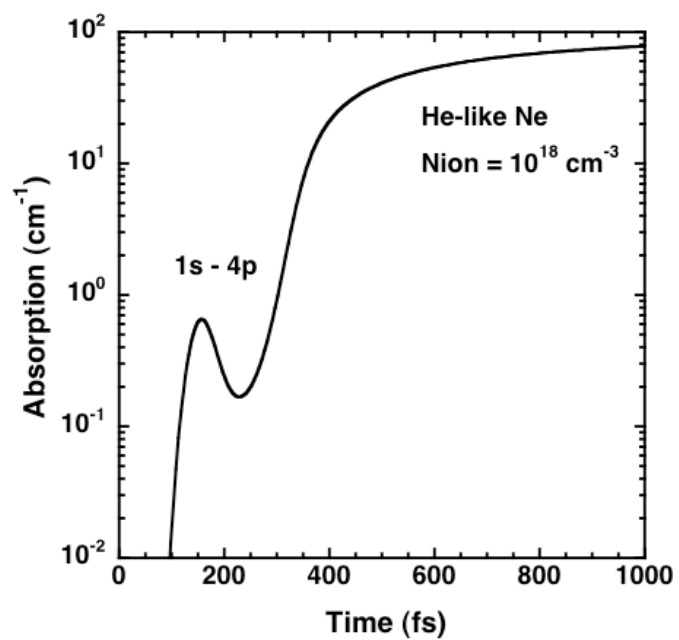


**Fig. 7.** Absorption coefficient of the 1s – 4p He-like Ne line that is photo-pumped versus time. The intensity of the X-FEL peaks at 200 fs on this time scale.